

V. A. EREMenko¹, Professor, Doctor of Engineering Sciences, prof.eremenko@gmail.com
 V. A. VINNIKOV¹, Head of Department Professor, Doctor of Physico-mathematical Sciences
 A. S. PUGACH¹, Associate Professor, Candidate of Engineering Sciences
 M. A. KOSYREVA¹, Post-Graduate Student

¹College of Mining, National University of Science and Technology—MISIS, Moscow, Russia

SUBSTANTIATION OF RIB PILLAR SIZES FOR ROCK SALT MINING IN VERTICAL CYLINDRICAL STOPES ARRANGED AT THE NODES OF REGULAR TRIANGULAR PATTERN

Introduction

The modern level of geotechnology for underground salt mining features highly mechanized and less labor-intensive operation due to the wide application of shearers [1, 2]. An avoidless charge for the high efficiency is unsafety of miners who should be present in the stoping area all the time, and high loss of economic reserves left in rib pillars, which reach 50–80% and still rise in proportion to the growing depth of mining.

Such situation and evident tendencies totally disagree with the present-day requirements of resource-saving and efficient nature management. For this reason and in view of the dominant and persistent growth of the depth of mining in mineral-promising sites, it is a critical task to find new and cardinal novel geotechnologies capable to ensure safety and completeness of extraction of economic mineral reserves using alternative methodological approaches and appropriate process equipment [3–6]. The simplest way to find an alternative is making a decision which is converse to the adopted practice.

For salt mining, a concept of an alternative nature-like geotechnology is proposed to ensure geomechanically well-founded minimization of mineral losses in pillars at the preserved geodynamic safety [6–11].

In this respect, it is fundamental that horizontal stoping is changed to upward or downward stoping in drilled vertical cylinder-shaped openings.

Natural biological systems possess structures that ensure high strength and stability at minimum amount and mass of materials [3, 4]. Such structures consist of an external envelope and an internal volume with numerous fine partitions, and spatial positions of the latter are governed by the directions of the external loads. Such structures are graminoid stems and mammals' bones which perceive vertical loading when in motion. In modern bionics, these structural solutions of nature were reproduced in the form of cellular constructions widely used in aircraft engineering (airplane wings), ship building (bulkheads), etc. [12].

The main features of such designs is that their compressive strength is achieved not due to the increased amount of substance in a load-bearing frame as in the room-and-pillar mining but owing to the high relative stiffness of an inner pattern governed by the geometry of cells, which, in its turn, is described by such parameters as circle diameter, shape and dimension of rib pillars etc.

In view of the above, the geomechanical validation of the stability of a cellular structure created in rock mass by drilling vertical cylindrical openings is an urgent task.

In the framework of Russian Science Foundation Project No. 19-17-00034 Natural-Technical Systems for Solid Mineral Mining Using Convergent Technologies, two designs are proposed for a honeycomb mine structure: 1—vertical cylindrical openings in bottom-up mechanized mining (Fig. 1); 2—vertical cylindrical openings in top-down mining by drilling with

The article presents a new geotechnical approach and a concept of an alternative convergent geotechnology for rock salt mining, which are based on the change of the mining front advance, namely, on the transition from horizontal stopes to ascending or descending vertical cylindrical stopes created by drilling. The rib pillar stability is calculated using the Turner–Shevyakov hypothesis for the conventional room-and-pillar mining and for the vertical cylindrical stopes with rib pillars with their corners cut off by circles. The analytical calculation procedure is developed for determining stability of structural elements in honeycomb mines, and the limitation conditions are defined for the Shevyakov method in case of the conventional and new-structure mines. The authors describe a variant of the stress–strain modeling in rib pillars with their corners cut off by vertical cylindrical stopes arranged in triangular patterns for the honeycomb structure mine at the depth of 1000 m. The procedure should further be adapted for the calculations of rib pillar parameters for honeycomb mines under different variants of the natural stress field: gravitational, lithostatic and gravitational–tectonic.

Keywords: The Turner–Shevyakov hypothesis, rib pillar, vertical cylindrical stopes, honeycomb mine structure, structural elements of mining system, strength factor SF , rock mass displacement, rock salt deposit

DOI: 10.17580/em.2023.02.12

reaming and using the reamed holes for bypassing broken minerals (Fig. 2) [5, 6].

The design of this system is used as a framework for the geomechanical substantiation of cylindrical openings in underground salt mining and for the optimization of their parameters to preserve stability of a honeycomb mine structure in different geological conditions.

Figures 1 and 2 depict mining systems with the square patterns of cells. Substantiation of the dimensions of rib pillars on condition of their stability in salt mining by vertical stopes of cylindrical shape and with the square pattern will be presented in *Gornyi Zhurnal* No. 1–2024.

The Turner–Shevyakov hypothesis for conventional room-and-pillar mining and for mining with vertical cylindrical stopes with rib pillars with their corners cut off by circles. analytical calculation procedures

The Turner hypothesis says that the pressure on the regular pillars is governed by the weight of the overlying rock column from the roof of a rib pillar to ground surface rested upon the area of rocks supported by the pillar [13–16]:

$$P = SH\gamma, \quad H, \quad (1)$$

where S is the horizontal area of the overlying rock surface applying pressure to a pillar (pillars) and supported by the pillar (pillars), m^2 ; H is the depth of the pillars below ground surface, m ; γ is the weighted average bulk density of overlying rocks, N/m^3 .

Shevyakov used the method of rib pillar design to determine that [13, 14]: the highest load is applied to support pillars by the weight of rock strata up to the ground surface; the vertical compression stresses are uniformly distributed in horizontal cross-sections of pillars and the pillar strength estimation uses the values of ultimate compressive strengths obtained experimentally on a laboratory scale. Such approach is admissible for ore bodies having the length greater than their occurrence depth. Otherwise, when

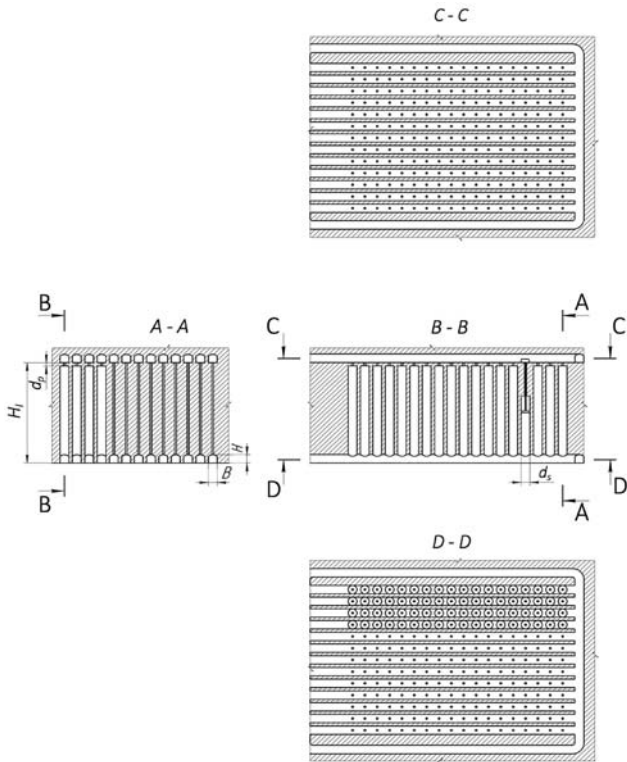


Fig. 1. Honeycomb system of bottom-up mechanized mining: H_l —height of level; B —width of horizontal development entries; H —height of horizontal development entries; d_s —diameter of cylindrical stope; d_p —height of crown pillar

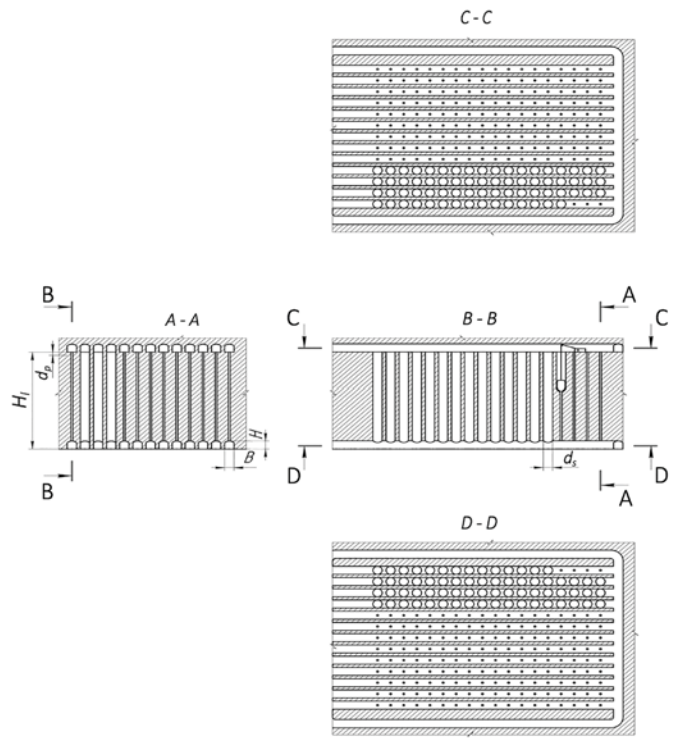


Fig. 2. Honeycomb system for top-down mining with drilling, reaming and using reamed holes for bypassing broken minerals to concentration level

the ore body length is smaller than the occurrence depth, the pressure on the rib pillars can be much lesser than the pressure due to the overlying rock weight.

The stability condition is given by:

$$P \leq F_{com}^{lim} - F_p^{res}, H, \quad (2)$$

where F_{com}^{lim} is the limit compression force ($F_{com}^{lim} = s_p R_p$), H ; F_p^{res} is the resistance of the pillar ($F_p^{res} = s_p h_p \gamma_p$), N ; s_p is the horizontal cross-section area of the pillar, m^2 ; h_p is the height of the pillar, m ; γ_p is the bulk density of rock in the pillar, N/m^3 ; R_p is the ultimate compressive strength of the pillar, N/m^2 .

Pillars are subjected to uniaxial compression. The actual nonuniformity of stresses [17, 18] is taken into account by introducing the strength factor of pillars.

With regard to the pillar strength factor n , we obtained from (2) that:

$$SH\gamma + s_p h_p \gamma_p \leq s_p R_p \frac{1}{n}, N. \quad (3)$$

Transformation of (3) yields:

$$\frac{S}{s_p} \leq \frac{R_p}{nH\gamma} - \frac{h_p \gamma_p}{H\gamma}. \quad (4)$$

This article discusses different variants of conventional room-and-pillar mining and novel vertical mining in cylindrical stopes with pillars with their corners cut off by circles (Fig. 3).

Variant 1. For columnar pillars between stopes $h_s \times d_s \times b_s$ (height \times length \times width), the pillar width a_p at the pillar length d_p is found from

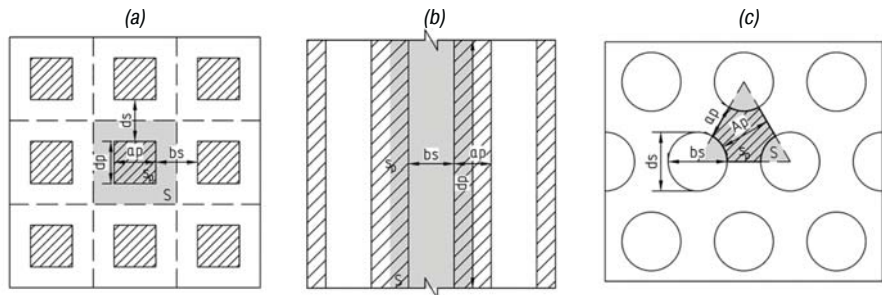


Fig. 3. Flow charts of room-and-pillar mining with columnar rib pillars (a), chain rib pillars (b) and with rib pillars with corners cut off by vertical cylindrical stopes in equilateral triangular pattern for honeycomb mine structure (c):

b_s —width of stope (for honeycomb structures, stope diameter $b_s = d_s$); d_s —length of stope (for honeycomb structures, stope diameter $d_s = b_s$); a_p —width of pillar (for honeycomb structures, minimum pillar width a_p , maximum pillar width A_p)

transformations of an expression derived from geometrical considerations (see fig. 3a):

$$\begin{aligned} \frac{S}{s_p} &= \frac{(b_s + a_p)(d_s + d_p)}{a_p d_p} = \frac{b_s d_s + b_s d_p + a_p d_s + a_p d_p}{a_p d_p} = \\ &= \frac{b_s d_s}{a_p d_p} + \frac{b_s}{a_p} + \frac{d_s}{d_p} + 1. \end{aligned} \quad (5)$$

Considering (5), condition (4) can be rewritten as follows:

$$\frac{b_s d_s}{a_p d_p} + \frac{b_s}{a_p} + \frac{d_s}{d_p} + 1 \leq \frac{R_p}{nH\gamma} - \frac{h_p \gamma_p}{H\gamma};$$

wherefrom:
$$a_p \geq \frac{\frac{b_s d_s}{d_p} + b_s}{\frac{R_p}{nH\gamma} - \frac{h_p \gamma_p}{H\gamma} - \frac{d_s}{d_p} - 1}, m. \quad (6)$$

In this manner, with regard to the pillar strength factor, the minimum width of a pillar:

$$a_p = \frac{b_s + \frac{b_s d_s}{d_p}}{\frac{R_p}{nH\gamma} - \frac{h_p \gamma_p}{H\gamma} - \frac{d_s}{d_p} - 1}, m. \quad (7)$$

Variant 2. For chain pillars ($d_p \rightarrow \infty$), expression (7) acquires the form of (see fig. 3b):

$$a_p = \frac{b_s}{\frac{R_p}{nH\gamma} - \frac{h_p \gamma_p}{H\gamma} - 1}, m. \quad (8)$$

Variant 3. For the variant of mining with vertical cylindrical stopes arranged in accordance with the equilateral triangular pattern (see fig. 3c), by analogy with the above calculations using formula (5), we obtain:

$$\begin{aligned} \frac{S}{s_p} &= \frac{\frac{l^2 \sqrt{3}}{4}}{\frac{l^2 \sqrt{3}}{4} - 3 \frac{\frac{\pi b_s^2}{360^\circ} \alpha}{4}} = \frac{(a_p + b_s)^2 \sqrt{3}}{4 \left(\frac{(a_p + b_s)^2 \sqrt{3}}{4} - \frac{\pi b_s^2}{8} \right)} = \\ &= \frac{(a_p + b_s)^2 \sqrt{3}}{(a_p + b_s)^2 \sqrt{3} - \frac{\pi b_s^2}{2}}, \end{aligned} \quad (9)$$

where l is the length of the side of the equilateral triangle, m , $l = (a_p + b_s)$; α is the angle of the sector cut off a pillar, for the equilateral triangle, this angle is 60° .

Considering (9), condition (4) is rewritten as follows:

$$a_p + b_s \geq \frac{\sqrt{\pi b_s}}{\sqrt[4]{3} \sqrt{2} \sqrt{1 - \frac{nH\gamma}{R_p - nh_p \gamma_p}}}. \quad (10)$$

We solve the obtained inequality:

$$a_p \geq \frac{\sqrt{\pi b_s}}{\sqrt[4]{3} \sqrt{2} \sqrt{1 - \frac{nH\gamma}{R_p - nh_p \gamma_p}}} - b_s, m. \quad (11)$$

Then, the width of the pillar is found from the formula:

$$a_p = -b_s + \frac{b_s}{\sqrt[4]{3}} \sqrt{\frac{\pi}{2 \left(1 - \frac{nH\gamma}{R_p - nh_p \gamma_p} \right)}}, m. \quad (12)$$

When the size of a pillar is expressed not in terms of the minimum width a_p but in terms of the maximum width A_p , then:

$$A_p = \frac{1}{2} \left(-b_s + b_s \sqrt[4]{3} \sqrt{\frac{\pi}{2 \left(1 - \frac{nH\gamma}{R_p - nh_p \gamma_p} \right)}} \right), m. \quad (13)$$

Let us compare formulas (7) and (13). The horizontal area of the overlying rock strata, S , which applies pressure to a pillar and is supported by the pillar, is bigger than the pillar area s_p since the calculation is added with the area of the mined-out voids around the pillar. For the variant of mining by vertical cylindrical stopes, the area of the surface of the overlying rock strata covers the area of the pillars and the areas of segments of the stopes surrounding the pillars, which in Variant 3 are the half of the area of one stope. The areas of segments of the vertical cylindrical stopes are taken into account as b_s . Entered in the numerator, this parameter includes the properties of a pillar and the summed area of segments of stopes. They can be represented by rectangular areas adjoining the lateral and corner parts of a pillar and going beyond, in case of the vertical cylindrical stopes — by their segments, making all together the half of the area of a circular stope, adjoining the corner part of a pillar and going beyond the area of the overlying strata.

Thus, the pillar stability substantiation in different design variants reduces to the comparison of the stope width b_s in case of the columnar pillar with the pillar strength and with the rock mass properties in case of the vertical cylindrical stopes, which vary greater than the width of stopes, which ensures higher stability of such design.

Results

The check calculation was performed for the geotechnical condition of Sol-Ilets Mine and for the physical and mechanical properties of rock salt from the Ilets deposit (Table 1). The pillar height was selected to be $h_p = 60$ m based on the potentiality of twinning two levels with the height $H_l = 30$ m (geotechnical condition of the test mine) and usability of drilling equipment.

Table 1. Physical and mechanical properties of Ilets salt

Parameter	Unit of measure	Value
Bulk density γ	MN/m ³	0.021
Uniaxial compression strength σ_c	MPa	35
Tension strength σ_t	MPa	1.5
Cohesion C	MPa	5.9
Elasticity modulus E	MPa	30000
Internal friction angle φ	°	66.6
Poisson's ratio ν	—	0.35

The analytical calculations of the chain pillar width a_p in Variant 2 for the conditions of Sol-Ilets Mine are compiled in Table 2 (see fig. 3b). The models of the vertical cylindrical stopes and different design elements of a stopping area in Variant 3 for the conditions of Sol-Ilets Mine are compiled in Table 3 (Figs. 3c and 4). The analytical calculations of the maximal and minimal widths of a rib pillar in variant 3 are given in Tables 4 and 5 (see figs. 3c and 4).

It follows from Table 2 (analytically calculated widths of chain pillars, a_p) that some of the pillar widths calculated from formula (7) proposed by Shevyakov assume negative values. The calculated width of a pillar should be a positive value. Let us find out when it takes place. The numerator in (7) is always positive in the problem formulation. Let us rewrite the denominator as an inequality to conform with the positive values:

$$\frac{R_p}{nH\gamma} - \frac{h_p \gamma_p}{H\gamma} - \frac{d_s}{d_p} - 1 > 0. \quad (14)$$

$$\frac{R_p}{nH\gamma} - \frac{h_p \gamma_p}{H\gamma} > \frac{d_s}{d_p} + 1. \quad (15)$$

In this fashion, the denominator is composed of two parts:

- 1) $\frac{R_p}{nH\gamma} - \frac{h_p \gamma_p}{H\gamma}$ determines the weight of the overlying strata which apply pressure to a pillar and the resistance of the pillar (due to the equilibrium of forces);
- 2) $\frac{d_s}{d_p} + 1$ is governed by geometrical parameters of a pillar and

Table 2. Analytical calculation of chain pillar width a_p in Variant 2 for Sol-Ilets Mine (see fig. 3b)

Calculation no.	Pillar depth below ground surface, H, m	Stope width b_s /stope length d_s , m	Pillar width a_p /pillar length d_p , m	Pillar height h_p , m	Calculated pillar width a_p , m						
					$n=1$	$n=2$	$n=3$				
1*	250**	28/250*	27/250**	30	5.147	12.962	26.246				
2				40	5.185	13.206	27.269				
3				50	5.223	13.460	28.374				
4				60	5.263	13.724	29.573				
1	400			28/250*	27/250**	30	9.255	28.714	95.969		
2						40	9.332	29.469	104.963		
3						50	9.411	30.266	115.817		
4						60	9.491	31.106	129.175		
1	600					28/250*	27/250**	30	16.632	88.395	-201.691
2								40	16.798	93.304	-180.072
3								50	16.968	98.791	-162.640
4								60	17.141	104.963	-148.284
1	1000	28/250*	27/250**					30	45.893	-133.369	-57.936
2								40	46.658	-127.305	-56.761
3								50	47.449	-121.769	-55.633
4								60	48.267	-116.694	-54.549

1*—actual geotechnical conditions in Sol-Ilets Mine
 250**—average length of stopes in the mine, m
 Application range of the analytical method—positive values of pillar widths

Table 3. Alternative models for vertical cylindrical stopes with different structural elements of stoping area in Variant 3 for Sol-Ilets Mine (model size (extraction panel or block) 60 × 60 × 60 m) (see figs. 3c and 4)

Model no.	Model volume, m ³	Horizontal area of model, m ²	Diameter (width, length) of stope, m	Minimal pillar width a_p /Maximal pillar width A_p , m	Distance between stopes in row (number of stopes in row along the width of the model)/distance between the rows of stopes from their centers (number of the rows of stopes along the length of the model), m	Number of stopes in model	Horizontal area of voids (stopes) in model, S_{ym} , m ²	Horizontal area of salt rock mass in model pillars, S_{ym} , m ²	Width of perimeter pillar (west–east, north–south are the sides of the model (fig. 4), m	Mineral loss in pillars, Π_{pm} , %
1	216000	3600	2	0.5/1.16	0.5 m (23 stopes (1 rows) – 22 stopes (2 rows))/2.16 m (26 stopes)	299 stopes (1 rows) + 286 stopes (2 rows) = 585 stopes	1836.9	1763.1	1.5 (west–east); 2 (north–south)	48.97
2			2	1/1.59	1 m (19 stopes (1 rows) – 18 stopes (2 rows))/2.59 m (22 stopes)	209 stopes (1 rows) + 198 stopes (2 rows) = 407 stopes	1277.98	2322.02	2 (west–east); 1.8 (north–south)	64.50
3			3	0.75/1.74	0.75 m (15 stopes (1 rows) – 14 stopes (2 rows))/3.24 m (17 stopes)	135 stopes (1 rows) + 112 stopes (2 rows) = 247 stopes	1745.05	1854.94	2.25 (west–east); 2.58 (north–south)	51.52
4			3	1.5/2.39	1.5 m (13 stopes (1 rows) – 12 stopes (2 rows))/3.89 m (14 stopes)	91 stopes (1 rows) + 84 stopes (2 rows) = 175 stopes	1236.37	2363.62	1.5 (west–east); 3.21 (north–south)	65.65
5			4	1/2.33	1 m (11 stopes (1 rows) – 10 stopes (2 rows))/4.33 m (13 stopes)	77 stopes (1 rows) + 60 stopes (2 rows) = 137 stopes	1720.72	1879.28	3 (west–east); 2.02 (north–south)	52.20
6			4	2/3.19	2 m (9 stopes (1 rows) – 8 stopes (2 rows))/5.19 m (11 stopes)	54 stopes (1 rows) + 40 stopes (2 rows) = 94 stopes	1180.64	2419.36	4 (west–east); 2.05 (north–south)	67.20
7			5	1.25/2.91	1.25 m (9 stopes (1 rows) – 8 stopes (2 rows))/5.41 m (10 stopes)	45 stopes (1 rows) + 40 stopes (2 rows) = 85 stopes	1668.12	1931.87	2.5 (west–east); 3.15 (north–south)	53.66
8			5	2.5/3.99	2.5 m (7 stopes (1 rows) – 6 stopes (2 rows))/6.49 m (9 stopes)	35 stopes (1 rows) + 24 stopes (2 rows) = 59 stopes	1157.87	2442.12	5 (west–east); 1.54 (north–south)	67.83
9			6	1.5/3.49	1.5 m (7 stopes (1 rows) – 6 stopes (2 rows))/6.49 m (8 stopes)	28 stopes (1 rows) + 24 stopes (2 rows) = 52 stopes	1469.52	2130.48	4.5 (west–east); 4.28 (north–south)	59.18
10			6	3/4.79	3 m (6 stopes (1 rows) – 5 stopes (2 rows))/7.79 m (6 stopes)	18 stopes (1 rows) + 15 stopes (2 rows) = 33 stopes	932.58	2667.42	4.5 (west–east); 7.52 (north–south)	74.09

Table 4. Analytical calculation of minimal pillar width a_p in Variant 3 for Sol-Ilets Mine (see figs. 3c and 4)

Calculation no.	Pillar depth below ground surface, H , m	Stope width b_s /stope length d_s , m	Pillar width a_p /pillar length d_p , m	Pillar height h_p , m	Calculated pillar width a_p , m		
					$n=1$	$n=2$	$n=3$
1	250	2	0.5	60	0.075	0.324	0.730
2		2	1		0.075	0.324	0.730
3		3	0.75		0.113	0.487	1.096
4		3	1.5		0.113	0.487	1.096
5		4	1		0.151	0.649	1.461
6		4	2		0.151	0.649	1.461
7		5	1.25		0.188	0.811	1.826
8		5	2.5		0.188	0.811	1.826
9		6	1.5		0.226	0.973	2.191
10		6	3		0.226	0.973	2.191
1	400	2	0.5	60	0.203	0.767	2.511
2		2	1		0.203	0.767	2.511
3		3	0.75		0.305	1.150	3.767
4		3	1.5		0.305	1.150	3.767
5		4	1		0.407	1.533	5.023
6		4	2		0.407	1.533	5.023
7		5	1.25		0.508	1.916	6.279
8		5	2.5		0.508	1.916	6.279
9		6	1.5		0.610	2.300	7.534
10		6	3		0.610	2.300	7.534
1	600	2	0.5	60	0.418	2.149	Starting from depth $H=600$ m downward, the allowable strength factor of pillar is limited by $n=0-2.4$
2		2	1		0.418	2.149	
3		3	0.75		0.627	3.224	
4		3	1.5		0.627	3.224	
5		4	1		0.835	4.299	
6		4	2		0.835	4.299	
7		5	1.25		1.044	5.374	
8		5	2.5		1.044	5.374	
9		6	1.5		1.253	6.448	
10		6	3		1.253	6.448	
1	1000	2	0.5	60	1.143	Starting from depth $H=1000$ m downward, the allowable strength factor of pillar is limited by $n=0-0.5$	
2		2	1		1.143		
3		3	0.75		1.714		
4		3	1.5		1.714		
5		4	1		2.285		
6		4	2		2.285		
7		5	1.25		2.856		
8		5	2.5		2.856		
9		6	1.5		3.428		
10		6	3		3.428		

Minimal width of pillars should be amended with regard to the impact of buckling for pillars with the width/height ratio less than 0.5. The most effective techniques are the numerical calculation methods

stopes (from the ratio of areas). This means that geometrical similarity is observed in each calculation. The minus sign shows that the selected widths of stope are too much relative to the pillar size. When we select the stope size commensurable with the pillar size, the calculated width of pillars grows together with the stability factor (formula (7)). These conclusions point at the limitedness of the method and formula: the possibility of the negative value of pillar width is neglected and no corrections are provided. In this case, it is expedient to analyze different parameters for pillars at different depths: for the target levels, these value can be positive, for the other levels—negative, which is illogical.

Similarly, we determine the positive-value width of a pillar in Variant 3 of the vertical cylindrical stopes. We use formula (13) with the radicand denominator expressed in terms of broken number and with setting condition of positive values:

$$1 - \frac{nH\gamma}{R_p - nh_p\gamma_p} > 0. \tag{16}$$

$$\frac{R_p}{nH\gamma} - \frac{h_p\gamma_p}{H\gamma} > 1. \tag{17}$$

Inequality (17) is similar to inequality (15) where there are two parts: the equilibrium of forces and the geometrical parameters of pillar. In case of the vertical cylindrical stopes, the geometrical parameters by default have no influence on the sign of the pillar width. This is analogous to Variant 2 of chain pillars ($d_p \rightarrow \infty$ by Shevyakov). So, in mining with the vertical cylindrical stopes, the logic-sensitive values (positive sign) are the pillar height h_p and the pillar depth below ground surface, H .

The numerical modeling results obtained using the officially accepted program Midas (Fig. 5), the physical stress-strain simulation in a rib pillar with the corners cut off by the vertical cylindrical stopes arranged in the equilateral triangular pattern for the honeycomb mine structure, and the in-situ observations of the circular cross-section openings showed their strong stability in different geological conditions of salt deposits. Moreover, the parameters of the structural elements in the honeycomb constructions make it possible to reduce mineral losses in rib pillar from 50–80% to 30–45%. At the moment, the research is being finalized, and the authors prepare reports and publications of the modeling and in situ observation data.

Figure 5 illustrates the numerical calculation of the maximal displacements in enclosing rock mass surrounding the vertical cylindrical stopes in the honeycomb structure mine. The maximal displacement has the value of 0.0147 m, which is within the standard (Table 6). The salt rock mass is stable, which is confirmed by the high rate of reliability of the input data since the rock mass is homogenous

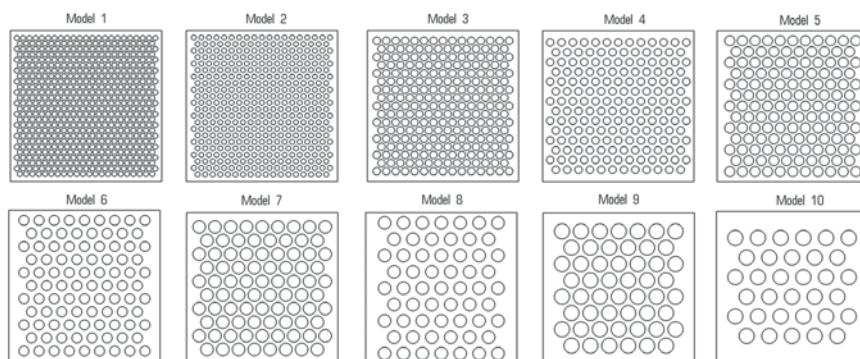


Fig. 4. Ten models with different-size structural elements (width of stopes and pillars) in stopping site (model size 60x60x60 m) (see table 3)

Table 5. Analytical calculation of maximal pillar width A_p in Variant 3 for Sol-Ilets Mine (see figs. 3c and 4)

Calculation no.	Pillar depth below ground surface, H, m	Stope width b_s /stope length d_s , m	Pillar width a_p /pillar length d_p , m	Pillar height h_p , m	Calculated pillar width a_p , m		
					n=1	n=2	n=3
1	250	2	2.5	60	0.797	1.013	1.365
2		2	3		0.797	1.013	1.365
3		3	3.75		1.196	1.520	2.047
4		3	4.5		1.196	1.520	2.047
5		4	5		1.595	2.026	2.729
6		4	6		1.595	2.026	2.729
7		5	6.25		1.993	2.533	3.412
8		5	7.5		1.993	2.533	3.412
9		6	7.5		2.392	3.039	4.094
10		6	9		2.392	3.039	4.094
1	400	2	2.5	60	0.908	1.396	2.907
2		2	3		0.908	1.396	2.907
3		3	3.75		1.362	2.094	4.360
4		3	4.5		1.362	2.094	4.360
5		4	5		1.816	2.792	5.814
6		4	6		1.816	2.792	5.814
7		5	6.25		2.270	3.490	7.267
8		5	7.5		2.270	3.490	7.267
9		6	7.5		2.724	4.188	8.721
10		6	9		2.724	4.188	8.721
1	600	2	2.5	60	1.094	2.593	Starting from depth H=600 m downward, the allowable strength factor of pillar is limited by n=0–2.4
2		2	3		1.094	2.593	
3		3	3.75		1.641	3.890	
4		3	4.5		1.641	3.890	
5		4	5		2.188	5.187	
6		4	6		2.188	5.187	
7		5	6.25		2.735	6.484	
8		5	7.5		2.735	6.484	
9		6	7.5		3.281	7.780	
10		6	9		3.281	7.780	
1	1000	2	2.5	60	1.722	Starting from depth H=1000 m downward, the allowable strength factor of pillar is limited by n=0–1.5	
2		2	3		1.722		
3		3	3.75		2.582		
4		3	4.5		2.582		
5		4	5		3.443		
6		4	6		3.443		
7		5	6.25		4.304		
8		5	7.5		4.304		
9		6	7.5		5.165		
10		6	9		5.165		

Table 6. Instability criterion of enclosing rock mass in numerical models

No.	Maximal displacement range [*] , m	Description
1	0.000–0.075	Low probability of deformation and collapse
2	0.076–0.140	Medium probability of deformation and collapse
3	0.0141–0.260	Probability of small-volume collapse
4	0.261–0.480	Probability of medium-volume collapse (SF** < 1.3–1.5)
5	0.481–>>>0.65	Probability of large-volume collapse (SF** < 1.2–1.3)

*Found from long-term in situ observation results
 **Allowable strength factor of pillars (in mine planning and design) in numerical analysis at high probability of input data is assumed to be SF ≥ 1.5

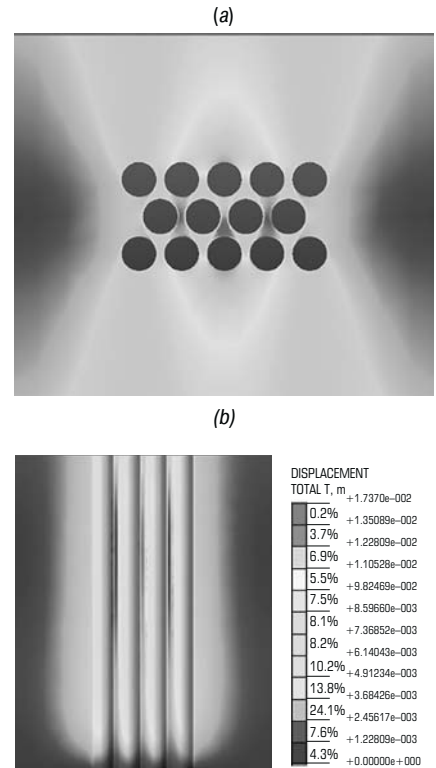


Fig. 5. Midas-based stress–strain analysis for honeycomb mine structure with maximal displacements in rock mass at the depth $H=1000$ m (a–horizontal section in the center of block/model $60 \times 60 \times 60$ m, b–vertical section). DISPLACEMENT TOTAL T–maximal displacement at the final stage of calculation: color spectrum (displacement range) 0.00000–0.0147 m

and uniform, and its physical and mechanical properties vary slightly with depth, and the natural stress state is lithostatic.

At the final stage of the research, analytical formulas (12) and (13) will be verified using the numerical modeling and physical simulation results.


Conclusions

The article has presented the analytical calculation procedure for the stability of rib pillars with corners cut off by circles for the conditions of the honeycomb mine structure with the vertical cylindrical stopes. The basis of the research is the hypothesis that the pressure applied to the regularly arranged pillars is governed by the weight of the column of overlying rock strata from the roof of a pillar to the ground surface rested on the area of rocks supported by the pillars.

The highest load on the support pillars is applied by the weight of the rock strata up to the ground surface: the vertical compression stresses are distributed uniformly in the horizontal cross-sections of the pillars, and the pillar strength calculation uses the ultimate strength values obtained experimentally in lab-scale compression tests. The stability of rib pillars with corners cut off by circles of the

vertical cylindrical stopes is ensured (as against the conventional columnar and chain pillars) by the ability of the pillars to have the lateral thrust with the neighbor pillars in the variant of the honeycomb mine structure, and by the most favorable shape of the structural elements of such mine—vertical cylindrical stopes which are sufficiently stable in the conditions of rock pressure (the effective stresses of the vertical cylindrical stopes flow around the rib pillars).

References

- Eremenko V. A., Kosyreva M. A., Vysotin N. G., Khazhy-ylai Ch. V. Geomechanical justification of room-and-pillar dimensions for rock salt and polyminer salt mining. *Gornyi Zhurnal*. 2021. No. 1. pp. 37–43.
- Zakharov V. N., Eremenko V. A., Fedorov E. V., Lagutin D. V. Geomechanical support of mine planning and design in the Iletsk rock salt field. *Gornyi Zhurnal*. No. 2. 2018. pp. 41–47.
- Trubetskoy K. N., Galchenko Yu. P. Nature-like geotechnology for integrated subsoil use : Problems and prospects. Moscow : Nauchtekhizdat, 2020. 368 p.
- Trubetskoy K. N., Galchenko Yu. P. Geoecology of subsoil use and eco-geotechnology of mineral mining. Moscow : Nauchtekhizdat, 2015. 360 p.
- Galchenko Yu. P., Eremenko V. A. Natural–technical systems of underground or mining using convergent technologies. Monograph. 2nd edition, extended and amended. Zakharov V. N. (Ed.). Moscow : Gornaya kniga, 2023. 288 p.
- Eremenko V. A., Myaskov A. V., Galchenko Yu. P., Romero Barrenechea Moisés Esau. Substantiation of convergent technology parameters for Ilets rock salt deposit. *Journal of Fundamental and Applied Problems of Mining Science*. 2018. Vol. 5. pp. 37–48.
- Zhengzheng Xie, Nong Zhang, Xiaowei Feng, Dongxu Liang, Qun Wei. et al. Investigation on the evolution and control of surrounding rock fracture under different supporting conditions in deep roadway during excavation period. *International Journal of Rock Mechanics and Mining Sciences*. 2019. Vol. 123. ID. 104122.
- Islavath S. R., Deb D., Kumar H. Development of a roof-to-floor convergence index for longwall face using combined finite element modelling and statistical approach. *International Journal of Rock Mechanics and Mining Sciences*. 2020. Vol. 127. pp. 204–221.
- Fei Wu, Hao Zhang, Quanle Zou, Cunbao Li, Jie Chen, Renbo Gao. Viscoelastic-plastic damage creep model for salt rock based on fractional derivative theory. *Mechanics of Materials*. 2020. Vol. 150. pp. 1–14. ID. 103600.
- Jianqiang Deng, Yaoru Liu, Qiang Yang, Wei Cui, Yinbang Zhu, Yi Liu, Bingqi Li. A viscoelastic, viscoplastic, and viscodamage constitutive model of salt rock for underground energy storage cavern. *Computers and Geotechnics*. 2019. Vol. 119. ID. 103288.
- Huang Xiao Lan, Chao Yu. Studies of hard interlayer's influence on the creep deformation of salt rock cavity. *Advanced Materials Research*. 2012. Vol. 594–597. pp. 452–455.
- Endogur A. I., Vainberg M. V., Ierusalimsky K. M. Honeycomb structure. Selection of parameters and design. Moscow : Mashinostroenie, 1986. 200 p.
- Shevyakov L. D. Calculation of strong dimension and deformation of support pillar. Moscow : AN SSSR, 1941. No. 7–9.
- Shevyakov L. D. Mineral mining. Moscow : Ugletekhizdat, 1953.
- Borshch-Kompaniets V. I. Practical geomechanics of rocks. Moscow : Gornaya kniga, 2013. 322 p.
- Gulevich G. E. Rational layouts and optimal sizes of support pillars in room-and-pillar mining. Moscow : OBNTI Giprotsvetmet, 1958.
- Mohr H. F. Measurement of rock pressure. *Mine and Quarry Engineering*. 1956.
- Nast N. The measurement of rock pressure in mines. *Sver. Geol. Unversokhr. Ser. C-Stokholm*. 1958. Vol. 52, No. 3. 183 p. 

UDC 622.234.42

E. Kh. ABEN¹, Associate Professor, Candidate of Engineering Sciences

Z. R. MALANCHUK², Professor, Doctor of Engineering Sciences

V. S. FEDOTENKO³, Deputy Science Director, Doctor of Engineering Sciences, victorfedotenko@gmail.com

B. A. ORYNBAEV¹, Candidate for a Doctor's Degree

¹Satbayev University, Almaty, Kazakhstan

²National University of Water and Environmental Engineering, Rovno, Ukraine

³Institute of Problems of Integrated Development of Mineral Resources, Moscow, Russia

IMPROVING EFFICIENCY OF ROCK BREAKING USING PRE-WEAKENING OF ROCK MASS

The purpose of this study is to improve the quality of drilling and blasting operations using pre-weakening of rock mass. The approach used in the study involved pilot testing of the pre-weakening technology efficiency at the Ayak-Kodzhan open pit in Kazakhstan. The testing plan included five blasts using the standard technology and five blasts with the pre-weakening technology with subsequent change in the drilling-and-blasting parameters toward their optimization for increasing the breaking efficiency. The K-MINE: Grain Size module (developed by K-MINE, Kryvyi Rih, Ukraine) was used to determine the granulometric composition of blasted rock mass and to assess the quality of fragmentation by blasting during rock excavation. In addition, the rate of rock mass loading to dump trucks, the bench bottom condition and the slope fracturing were evaluated.

Keywords: ore breaking, explosive, fragmentation quality, pre-weakening, blasthole efficiency ratio, burden

DOI: 10.17580/em.2023.02.13

Introduction

Although significant progress has been made in the scientific and technical aspects of rock fracture by blasting, many mining companies pursue improvement of blasting efficiency.

Despite advancements in the blasting technique and industrial explosives, the technical and economic characteristics of explosives somewhat fall behind the growing demands of the mining industry. Blasting accounts for up to 30%

of mineral mining costs as a dominant method of fracturing large volumes of rocks. Crushing and milling are among the highest energy-consuming processes and take up to 30–60% of total energy consumption. The quality of blasting and rock fragmentation by blasting are crucial for subsequent ore processing, and are a determining factor for various technological and economic indicators.

A feature of many deposits is the variability of the physical and mechanical properties of rocks across both an area of an open pit field and a volume